Analyzing Free Energy Relationships for Proton Translocations in Enzymes: Carbonic Anhydrase Revisited

C. N. Schutz and A. Warshel*

Department of Chemistry, University of Southern California, Los Angeles, California 90089-1062

Received: September 1, 2003; In Final Form: November 21, 2003

The nature of proton transfer (PT) in proteins is explored by considering the catalytic cycle of carbonic anhydrase III. Special attention is paid to the free energy relationship established by Silverman and co-workers (Silverman, D. N.; Tu, C.; Chen, X.; Tanhauser, S. M.; Kresge, A. J.; Laipis, P. J. *Biochemistry* **1993**, *34*, 10757−10762). The free energy surfaces for the PT process is analyzed in the framework of the modified Marcus theory of Warshel and co-workers (Warshel, A.; Hwang, J. K.; Åqvist, J. *Faraday Discuss.* **1992**, *93*, 22), using realistic values of the relevant reorganization energy and the off-diagonal mixing term. It is found that the free energy relationship reflects a much more complex situation than that deduced from an empirical fit to the standard two-state Marcus formula. Apparently, the PT process involves three or more parabolic free energy surfaces rather than the two assumed in the Marcus treatment. Furthermore, PT processes involve large off-diagonal mixing terms that lead to apparent reorganization energies which are much smaller than the actual reorganization energies. Because our analysis reproduced the experimental trend using nonadjustable molecular parameters (derived by actual molecular simulations), we believe that this analysis is much more consistent than alternative phenomenological fitting approaches. The present approach provides a general framework for studies of proton translocations in proteins and justifies the approach used in our recent study of proton transport in bacterial reaction centers and aquaporin.

I. Introduction

Linear free energy relationships (LFERs), or free energy relationships (FERs) if one considers large changes in free energy, have provided a powerful way of correlating rates and energetics of chemical reaction in solutions.[1−6] The validity of LFERs has been widely accepted because many reactions follow such relationships[3−5] and in part because theoretical studies have lent a strong support for their general validity (e.g., refs 7−11). It has been demonstrated that such relationships are also useful in studies of enzymatic reactions.[1,2,10,12−19,21] Some recent studies of LFERs in enzymes have involved the use of a Marcus-type relationship and attempt to draw molecular information from such relationships. This coincided with attempts to analyze the possible relationship between the so-called reorganization energy (λ) and the catalytic effect of enzymes.[1,14,16,20] Some workers argued that enzyme catalysis is manifested by reduction of the free energies of high-energy intermediates,[20] while others argued that catalytic effects were associated with the reduction of λ.[16]

Earlier theoretical works[10,15] provided detailed analysis of LFERs in enzymes and pointed out that the use of a simple Marcus relationship,[7] which is based on two intersecting parabolas, might not capture the actual LFERs in enzymes. The reason for this problem is associated in part with the fact that most reactions involve transfer between more than two valence bond states. Furthermore, the proper description of chemical reactions involves large mixing terms, which are not considered in most Marcus-like treatments. At any rate, quantitative attempts to analyze LFERs in enzymes have remained quite limited.

LFERs provide a very useful way of studying proton transfer (PT) reactions in proteins[1,9,10,22] and in modeling proton translocations (PTR).[23] An ideal system to examine the validity of LFERs in proteins is human carbonic anhydrase III (which will be referred to here as CA III).[1] This and other CAs are so useful because they involve a series of PT processes where the proton is moved from the catalytic water to the bulk water (see also below) and thus can serve as a benchmark for models of proton shuttles in proteins. This benchmark includes the instructive findings of Silverman and co-workers,[1,17] who demonstrated that the rate of PT in mutants of CA III is correlated with the pK_a difference between the donor and acceptor. This work[1,17] demonstrated that the observed LFER follows a Marcus-type relationship. However, the uniqueness of the parameters that were used in the fitting process has not been established (see also below).

The present work reexamines the above experimental information by using a more rigorous theoretical description, combined with calculations of the relevant reorganization energies. It is shown that the new treatment leads to an interpretation which is more consistent with the structure of CA III and with the availability of several PT steps; it is concluded that the reorganization energy cannot be deduced in a unique way from Marcus-like treatment of the observed LFER and that combining theory and experimental information can lead to a much more consistent analysis of LFERs in enzymes. We also provide a general analysis about the nature of PT in CA and related systems.

II. Background

The catalytic reaction of CA III has been subjected to extensive studies (e.g., refs 24−26). The structural elements of

* Author to whom correspondence should be addressed. Phone: 213 740-4114. Fax: 213 740-2701. E-mail: warshel@usc.edu.

10.1021/jp0366015 CCC: $27.50
Published on Web 01/16/2004

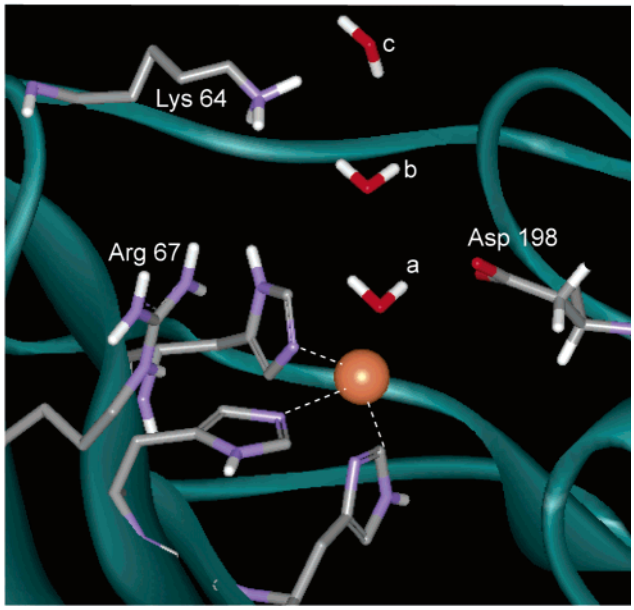

Figure 1. The active site of the F198D mutant of CA III, showing the three histidine ligands: His-94, His-96, and His-119. Also shown are residues Lys-64 and Arg-67 and the Asp residue at position 198 (this residue corresponds to Phe-198 in the native enzyme).

the enzyme that will be discussed here are depicted in Figure 1. They include an active site Zn^{2+} and a chain of proton transport elements, which connects the solution phase to the Zn^{2+} center. The catalytic process of this system is described traditionally[27] in terms of two steps. The first is attack of a zinc-bound hydroxide on CO_2,[28]

$$CO_2 + EZn^{2+}(OH^-) + H_2O \leftrightarrows HCO_3^- + EZn^{2+}(H_2O) \quad (1)$$

The reversal of this reaction is called the "dehydration step". The second step involves the regeneration of the OH^- by a series of PT steps[25,29]

$$EZn^{2+}(H_2O) + B \underset{k_B}{\overset{k_{-B}}{\rightleftharpoons}} EZn^{2+}(HO^-) + BH^+ \quad (2)$$

where $K_{-B} = k_{-B}/k_B$ (in the notation of ref 1) and BH^+ can be water, buffer in solution, or the protonated form of Lys64 (other CAs have His in position 64). Previous experimental studies[1] have established an FER that was fitted to the Marcus equation using

$$\Delta g^{\ddagger} = w^r + \{1 + \Delta G^0/4\Delta G_0^{\ddagger}\}^2 \Delta G_0^{\ddagger} \quad (3)$$

where the observed reaction free energy is given by $\Delta G^0_{obs} = w^r + \Delta G^0 - w^p$, where w^r is the work of bringing the reactants to their reacting configuration and w^p is the corresponding work for the reverse reaction. ΔG^0 is the free energy of the reaction when the donor and acceptor are at their optimal distance. $\Delta G_0^{\ddagger}$ is the so-called intrinsic activation barrier which is actually $^1/_4$ of the corresponding reorganization energy λ. Here we use $\Delta g^{\ddagger}$ rather than $\Delta G^{\ddagger}$ for the activation barrier following the consideration of ref 10. Equation 3 can also be written in the well-known form

$$\Delta g^{\ddagger} = w^r + (\Delta G^0 + \lambda)^2/4\lambda \quad (4)$$

The phenomenological fitting processes yielded $\lambda = 5.6$ kcal/mol and $w^r \cong 10.0$ kcal/mol. The estimated value of λ appears to be in conflict with the value deduced from computer simulation studies ($\lambda \cong 80$ kcal/mol in ref 2). Furthermore, the large value of w^r is hard to rationalize since the reaction involves a proton transfer between a relatively fixed donor and acceptor (residue 64 and the zinc-bound hydroxide). The very small values of λ obtained by fitting eq 4 to experiment are not exclusive to CA III. Similarly, small values were obtained in the analysis of other enzymes and are drastically different than the values obtained by actual microscopic computer simulations (note in this respect that λ cannot be measured directly).

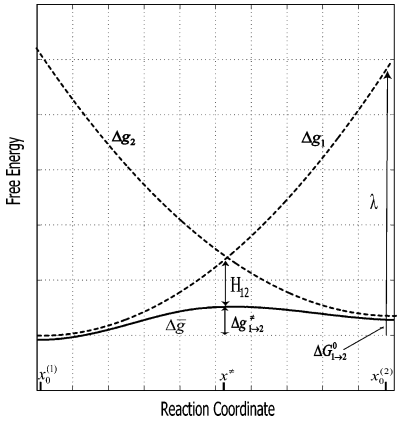

Figure 2. Relationship between the diabatic free energies (the Δg_i's) and the adiabatic ground state free energy ($\Delta\bar{g}$) in a two-state EVB model. The figure depicts the diabatic and adiabatic free energy surfaces by (- - -) and (—), respectively, as well as the reorganization energy (λ) and the off-diagonal term (H_{12}).

As pointed out before,[15,22,30] the above discrepancies reflect the following problems: First, the reaction under study may involve more than two intersecting parabolas and thus cannot be described by eq 4. Second, although eq 4 gives a proper description for electron transfer (ET) reactions where the mixing between the reactant and product state (H_{12}) is small, it cannot be used for describing proton transfer or other bond-breaking reactions, where H_{12} is large. In such cases one should use an expression referred to as the Hwang Åqvist Warshel (HAW) expression[2,31]

$$\Delta g^{\ddagger} = w^r + (\Delta G^0 + \lambda)^2/4\lambda - \bar{H}_{12}(x^{\ddagger}) + \frac{\bar{H}_{12}(x_0)^2}{(\Delta G^0 + \lambda)} - \Gamma \quad (5)$$

where Γ is the nuclear quantum mechanical correction and the $\bar{H}_{12}$ are the average values of H_{12} in the transition state ($x^{\ddagger}$) and the reactant state (x_0). The nature of the parameters in this expression is illustrated schematically in Figure 2 (a more systematic discussion is given in section III). It is useful to note in this respect that the first term in this expression is the regular Marcus equation,[32] which corresponds to the intersection of Δg_1 and Δg_2 at $x^{\ddagger}$. The second and third terms represent, respectively, the effect of H_{12} at $x^{\ddagger}$ and $x_0^{(i)}$.

For further analysis we will also consider the zero-order (diabatic) activation barrier obtained from the intersection of the zero-order diabatic state. That is, we will also consider

$$(\Delta g^{\ddagger})_{di} = (\Delta G^0 + \lambda)^2/4\lambda \quad (6)$$

The changes in the actual adiabatic barrier ($\Delta g^{\ddagger}$) are correlated linearly with the changes of the diabatic barrier $(\Delta g^{\ddagger})_{di}$ and with the changes of ΔG^0 (see ref 10 and the next section). This can be expressed by

$$\frac{\Delta\Delta g^{\ddagger}}{\Delta\Delta G^0} \cong \frac{(\Delta g^{\ddagger})_{di}}{\Delta\Delta G^0} \approx \theta \quad (7a)$$

where $\Delta\Delta g^{\ddagger}$ and $\Delta\Delta G^0$ are the changes in $\Delta g^{\ddagger}$ and ΔG^0, respectively. Thus we obtain

$$\Delta\Delta g^{\ddagger} \cong \theta\Delta\Delta G^0 \tag{7b}$$

Apparently, the fact that the use of eq 5 is an essential element of a proper treatment of PT reactions is not so widely recognized in the biochemical community. In fact, some readers of this work demanded an "experimental" proof for the need of eq 5. Such a requirement would be reasonable for phenomenologically based equations, but it is less justified for equations that are obtained from fully microscopic approaches (see, for example, our illustration of the validity of the Marcus formula for electron transfer reactions[33]). In fact, the requirement for an experimental verification of the HAW relationship is equivalent in some respects to the requirement of an experimental proof for the validity of the quadratic equation. At any rate, we provide in the next section a detailed derivation of eq 5.

III. Theoretical Approaches

Theoretical studies of PT in condensed phases require clear molecular models and cannot be based on the use of phenomenological models with phenomenologically determined parameters. In principle, one can use a combined quantum mechanics/molecular mechanics (QM/MM) molecular orbital approach (for review see ref 34). However, at present we believe that the most effective conceptual and computational approach is provided by the empirical valence bond (EVB) model[10,22,35−38] that has been used before in simulations of PT in enzymes[10,22,28] and in solution.[37,38] Although we will not use here the explicit EVB formulation, we will discuss this approach in order to establish a rigorous base to our modeling approach.

The EVB method describes the potential energy surface and charge distribution of the quantum system embedded in a specific environment (e.g., protein) in terms of diabatic states with the proton attached to different protonation sites. These states are then mixed by the appropriate off-diagonal terms. Here we consider for simplicity a "quantum" system of two water molecules and one proton embedded in a given environment. This system can be described by considering two states:

$$\begin{aligin}
\psi_1 &= (H-O_a-H)^{+}\ \ (O_b-H) \\
\psi_2 &= (H-O_a)\ \ (H-O_b-H)^{+}
\end{aligin} \tag{8}$$

The energies of these states in their specific environments are described by (e.g., ref 36)

$$\begin{aligin}
H_{11} &= \epsilon_1 = \epsilon_S^{(1)} + U_{sS}^{(1)} + U_{ss} \\
H_{22} &= \epsilon_2 = \epsilon_S^{(2)} + U_{sS}^{(2)} + U_{ss}
\end{aligin} \tag{9}$$

where S and s designate, respectively, the quantum system (the "solute") and the surrounding "solvent". The term $\epsilon_S^{(i)}$ is described by Morse potentials, a bond angle term, and a nonbonding interaction term that describes the interactions between the solute atoms in the ith state and the solvent molecules, while U_{ss} is the solvent−solvent force field. Now, the ground state potential surface is obtained by solving the secular equation:

$$HC_g = E_gC_g \tag{10}$$

In the simple two-states case we have

$$E_g = \frac{1}{2}[(\epsilon_1 + \epsilon_2) - \sqrt{(\epsilon_1 - \epsilon_2)^2 + 4H_{12}^2}] \tag{11}$$

In cases with more states (e.g., three water molecules) we have to solve a multistate Hamiltonian as was done repeatedly in EVB treatment (e.g., refs 10, 35, 37, and 38). The solution of eq 3 provides the eigenvector, C_g, and the corresponding charge distribution. This distribution may correspond to a localized picture where the proton charge is localized on one water molecule or to the case where the proton charge is delocalized. Now the EVB/umbrella sampling procedure (e.g., ref 10) allows one to obtain the rigorous profile of the free energy function $\Delta\bar{g}$ that corresponds to E_g and the free energy functions Δg_1 and Δg_2 that correspond to ϵ_1 and ϵ_2, respectively (see Figure 2). It is important to point out here that such profiles have been evaluated quantitatively in many EVB simulations of PT in proteins (for reviews see refs 34 and 36). The corresponding profiles provide the activation free energy $\Delta g^{\ddagger}$ for the given PT step. The calculated activation barrier can then be converted (e.g., see ref 10) to the corresponding rate constant using transition state theory (TST):

$$k_{ij} \cong (RT/h)\exp\{-\Delta g^{\ddagger}_{i\rightarrow j}/RT\} \tag{12}$$

A more rigorous expression for $k_{i\rightarrow j}$ can be obtained by multiplying the TST expression by a transmission factor that can be calculated easily by running downhill trajectories.[10] However, the corresponding correction is usually small[39] and will not change the conclusions of the present work. In any case, the calculated rate constant can now be used in calculations of proton transport processes.

At this point it is useful to consider the approximated expression for $\Delta\bar{g}$ and $\Delta g^{\ddagger}$. Here we note that with the simple two-state model of eq 11 we can obtain a very useful approximation to the $\Delta\bar{g}$ curve. That is, using the above-mentioned free energy EVB/umbrella sampling formulation, we obtain the $\Delta\bar{g}$ that corresponds to the E_g and the free energy functions Δg_i that correspond to the ϵ_i surfaces. This leads to the approximated expression

$$\Delta\bar{g}(x) = \frac{1}{2}[(\Delta g_1(x) + \Delta g_2(x)) - \sqrt{(\Delta g_1(x) - \Delta g_2(x))^2 + 4H_{12}^2(x)}] \tag{13}$$

where x is the generalized reaction coordinate, which is given by $\epsilon_1 - \epsilon_2$. This relationship can be verified in the case of small H_{12} by considering our ET studies,[33] whereas for larger H_{12} one should use a perturbation treatment. Now we can exploit the fact that the Δg_i curves can be approximated by parabolas of equal curvatures (this approximated relationship was found to be valid by many microscopic simulations (e.g., ref 36). This approximation can be expressed as

$$\Delta g_i(x) = \lambda\left(\frac{x - x_0^{(i)}}{x_0^{(j)} - x_0^{(i)}}\right)^2 \tag{14}$$

where λ is the so-called "solvent reorganization energy" (which is illustrated in Figure 2).

Using eqs 13 and 14 or the equivalent graphical representation of eq 2, one obtains our HAW equation, eq 5, which is given in the general case by

$$\Delta g^{\ddagger}_{i\rightarrow j} = (\Delta G^{0}_{i\rightarrow j} + \lambda_{i\rightarrow j})^2/4\lambda - \bar{H}_{ij}(x^{\ddagger}) + \bar{H}_{ij}{}^2(x_0^{(i)})/(\Delta G^{0}_{i\rightarrow j} + \lambda_{i\rightarrow j}) \quad (15)$$

where $\Delta G^{0}_{i\rightarrow j}$ is the free energy of the reaction, and $\bar{H}_{ij}(x^{\ddagger})$ and $\bar{H}_{ij}{}^2(x_0^{(i)})$ are the average values of H_{ij} at the transition state, $x^{\ddagger}$, and at the reactant state, $x_0^{(i)}$.

Repeated quantitative EVB studies of reactions in solutions and proteins (e.g., refs 13 and 36) established the quantitative validity of eq 15. With this fact in mind we can take these equations as a quantitative correlation between $\Delta g^{\ddagger}_{i\rightarrow j}$ and ΔG^0. Basically, when the changes in ΔG^0 are small, we obtain a linear relationship between $\Delta g^{\ddagger}_{i\rightarrow j}$ and ΔG^0. This linear relationship, which can be obtained by simply differentiating the $\Delta g^{\ddagger}_{i\rightarrow j}$ of eq 15 with respect to $\Delta G^{0}_{i\rightarrow j}$, can be expressed in the form of eq 7 (where $\theta = (\Delta G^{0}_{i\rightarrow j} + \lambda)/2\lambda$), once we neglect the contribution from the last term of eq 15. The linear correlation coefficient depends on the magnitude of ΔG^0 and λ. At any rate, more details about this linear free energy relationship (LFER) and its performance in studies of chemical and biochemical problems are given elsewhere.[6,10,18,31,36,40,41]

As much as the present work is concerned, the main point of eq 15 and Figure 2 is that the $\Delta G^{0}_{i\rightarrow j}$, which determines the corresponding $\Delta g^{\ddagger}_{i\rightarrow j}$, is correlated with the difference between the two minima of the $\Delta\bar{g}$ profile that correspond to states *i* and *j*, respectively.

With the above considerations in mind, we adopt here the strategy developed in our early studies of biological PTR[23,42,43] and combine semimacroscopic electrostatic calculations with the EVB conceptual picture. This is done by evaluating first the free energy of transferring the proton between two sites and then using the HAW expression for the activation barrier and the corresponding rate of PT between the sites. The main ingredients of this approach are described below.

The key parameter in eq 15 is the $\Delta G^{0}_{i\rightarrow j}$, and our task is to evaluate this parameter by converting the protein structure information to the energetics. Here we start formulating the energetics of all possible proton configurations (protons on different water molecules and/or on the protein residues) using[44]

$$\Delta G^{(m)} = \sum_i \{-2.3RTq_i^{(m)}[\mathrm{p}K_{\mathrm{int}}^{\mathrm{p}} - \mathrm{pH}] + 1/2\sum_{i\neq j} W_{ij}q_i^{(m)}\, q_j^{(m)}\} \quad (16)$$

where *m* designates the vector of the charge states of the given configuration [i.e., $m = (q_1^{(m)}, q_2^{(m)}, \cdots, q_n^{(m)})$]. Here, $q_i^{(m)}$ is the actual charge of the *i*th group (e.g., hydronium ion) at the *m*th configuration. This can be 0 or −1 for acids and 0 or 1 for bases (where we restrict our formulation to monoions, although the extension to $|q| > 1$ is trivial). The $W_{ij}q_iq_j$ term represents the effect of the interaction between the ionized residues. The intrinsic pK_a (pK_{int}) is the pK_a that the given ionizable group would have if all other ionizable groups were kept at their neutral state (the evaluation of this term is described in ref 44).

Now, the $\Delta G^{(m)}$ values can be converted to the corresponding energy of protonating the different sites. This can be obtained by[45]

$$\Delta G_{\mathrm{H}^+} = \sum_i \Delta G_{\mathrm{H}^+}{}^{(m,i)} = \sum_i (\Delta G^{(m)})_i\, q_i^m \quad (17)$$

where ΔG_{H^+} is the free energy of the given proton configuration, and $(\Delta G^{(m)})_i$ is the contribution to eq 16 from its *i*th term. In more explicit form, we can write

$$\Delta G^{m,i}_{\mathrm{H}^+}(\mathrm{B}_i \rightarrow \mathrm{B}_i\mathrm{H}^+) = -2.3RT[\mathrm{p}K_{\mathrm{a}}^{\mathrm{w}}(\mathrm{B}_i\mathrm{H}^+) - \mathrm{pH}] + (\Delta\Delta G_{\mathrm{sol}}^{\mathrm{w}\rightarrow\mathrm{p}}(q_i^{(m)}))_0 + \sum_{j\neq i} W_{ij}\, q_i^{(m)}\, q_j^{(m)} \quad (18)$$

where B_i designates the *i*th base, and $\Delta\Delta G_{\mathrm{sol}}^{\mathrm{w}\rightarrow\mathrm{p}}$ designates the change in the solvation free energy of BH^+ upon transfer from water to the specific protein site.

The key parameters in eqs 15 and 16 are the change in solvation free energies: $\Delta G_{\mathrm{sol}}^{\mathrm{w}\rightarrow\mathrm{p}}(q_i^{(m)})$. The calculations of these parameters are accomplished by using the semimicroscopic version of the protein dipoles Langevin dipoles (PDLD/S) method.[44,46] The effect of the protein reorganization is considered explicitly in these calculations by using the linear response approximation (LRA) and evaluating the PDLD/S energies for the charged and uncharged states of the relevant residues. For more details of the PDLD/S−LRA method, see refs 44 and 46. The charge−charge interaction term W_{ij} can be calculated in an explicit way (see refs 44 and 46). However, in most cases, we obtain good results by using

$$W_{ij} = 332/(r_{ij}\epsilon_{ij}) \quad (19)$$

where r_{ij} is the distance between the interacting groups and ϵ_{ij} is an effective dielectric constant whose value is determined by a distance dependent function.[46,47] The justification of this approximation is discussed in detail elsewhere.[44,46,48] Basically, ϵ_{ij} for charge−charge interaction reflects the compensation of the gas phase Coulombic interaction between the charges by the solvation effect of the protein plus solvent system. This compensation has been found to be unexpectedly large even for charge−charge interaction in the protein interior, leading to a large effective ϵ_{ij} (between 20 and 40). This fact has been established repeatedly by both theoretical and experimental studies (e.g., refs 49 and 50). It is also important to realize that ϵ_{ij} is not equal (and is typically much larger) than the dielectric constant ϵ_{p} that determines $\Delta\Delta G_{\mathrm{sol}}^{\mathrm{w}\rightarrow\mathrm{p}}$ (see ref 48).

Using the formulation of eq 18 to describe a PT between two bases gives

$$\begin{aligned}\Delta\Delta G(\mathrm{B}_i\mathrm{H}^+ + \mathrm{B}_{i+1} \rightarrow \mathrm{B}_i + \mathrm{B}_{i+1}\mathrm{H}^+) &= -2.3RT[\mathrm{p}K_{\mathrm{a}}^{\mathrm{w}}(\mathrm{B}_{i+1}\mathrm{H}^+) - \mathrm{p}K_{\mathrm{a}}^{\mathrm{w}}(\mathrm{B}_i\mathrm{H}^+)] + \\ &\Delta\Delta G_{\mathrm{sol}}^{\mathrm{w}\rightarrow\mathrm{p}}(\mathrm{B}_{i+1}\mathrm{H}^+)_0 - \Delta\Delta G_{\mathrm{sol}}^{\mathrm{w}\rightarrow\mathrm{p}}(\mathrm{B}_i\mathrm{H}^+)_0 + \Delta\Delta G_{i,i+1} \\ &= 2.3RT[\mathrm{p}K_{\mathrm{a}}^{\mathrm{p}}(\mathrm{B}_i\mathrm{H}^+) - \mathrm{p}K_{\mathrm{a}}^{\mathrm{p}}(\mathrm{B}_{i+1}\mathrm{H}^+)] + \Delta\Delta G_{i,i+1}\end{aligned} \quad (20)$$

where $\Delta\Delta G_{i,i+1}$ represents the change in interaction between the *i* and $i + 1$ group upon PT.

The PDLD/S−LRA calculations involved two levels of simulations. In the first step we performed explicit all-atom MD simulations with the surface-constrained all-atom solvent (SCAAS)[51] and the local reaction field (LRF) long-range treatment[52] to generate protein configurations with the charged and uncharged forms of the solute. In the next step we performed the PDLD/S calculations on the generated configuration and took their average as the consistent estimate of the self-energy. These two sets of calculations involved two different simulation systems and different boundary conditions. The first system is an all-atom system constructed by taking the H_3O^+ ion under consideration (or the protonated base under consideration) and then constructing an SCAAS simulation sphere around this ion and including in the system (in addition to the centered ion) the protein and the water molecules within 24 Å from the center.

Long-range effects were treated by the LRF approach. The all-atom simulations were used to generate 10 configurations for the charged and uncharged states. Each of these simulations was run for 2 ps at 300 K, starting from the previous configurations. The configurations generated by the all-atom simulations were used in the PDLD/S−LRA calculations. This simulation system involved a spherical system of a radius of 24 Å around the specific position of the protonated base under study. The protein was treated with $\epsilon_p = 4$, which is justified once we use the LRA approach. The PDLD/S sphere was surrounded by a continuum with $\epsilon = \epsilon_w$. The PDLD/S calculations were averaged over the above-mentioned configurations of the charged and uncharged states as required by the LRA procedure.

All the self-energy calculations were done with the program MOLARIS, which combines the ENZYMIX and POLARIS programs.[46] The MD simulations (needed to generate the protein configurations) were performed by the ENZYMIX module with the parameter set of ref 46, which included the effect of the induced dipoles.

The actual free energy of H_3O^+ in the *i*th site should also reflect the effect of the ionizable groups of the protein. This contribution was evaluated by the W_{ij} term of eq 9 with the ϵ_{ij} of ref 48. The ionization states of the protein groups at pH = 7.0 were evaluated by calculating the corresponding apparent pK_a's. These calculations were started by using the PDLD/S−LRA to find the intrinsic pK_a of each ionized residue and then using a self-consistent hybrid approach.[44]

All the PDLD/S−LRA simulations started by using the X-ray structure of CA III (PDB ID code 1FLJ[53]) and running relaxation trajectories of 50 ps. However, in studying specific mutants we generated first the given mutant by changing the native residue to the appropriate mutant residue and then running a long (100 ps) relaxation run. The internal water molecules were generated in all the available protein cavities using the standard MOLARIS procedure. Note, however, that the PDLD/S−LRA calculations replace by Langevin dipoles all water molecules, except the explicit water molecules considered in eq 21 of the next section.

IV. Reanalyzing the LFER of CA III

To obtain a proper molecular description of LFERs, it is essential to represent each reactant, product, or intermediate by a parabolic free energy function.[10] In the case of CA III, we describe the proton transfer from residue 64 (Lys or His) to the zinc-bound hydroxyl via a bridging water molecule (and alternatively two water molecules), by considering the three states

$$\begin{aligned}\psi_1 &= BH^+(H_2O)_b(OH^-)_aZn^{+2}\\ \psi_2 &= B(H_3O^+)_b(OH^-)_aZn^{+2}\\ \psi_3 &= B(H_2O)_b(H_2O)_aZn^{+2}\end{aligned} \quad (21)$$

where we denote by B the base at residue 64 and where ψ_1 and ψ_3 correspond, respectively, to the right and left sides of eq 2. The relative free energy of these states can be estimated from the corresponding pK_a's, where the pK_a's of $(H_2O)_a$ and B are known from different mutations,[1] while the pK_a of $(H_2O)_b$ can be calculated by the PDLD/S−LRA approach. Note that our three-state system can be easily extended to include one more water molecule and one more state. At any rate, using the relevant pK_a we can evaluate the free energy for a proton transfer (PT) between a donor (D) to an acceptor (A) using eq 20 (see also ref 54), which can be expressed as

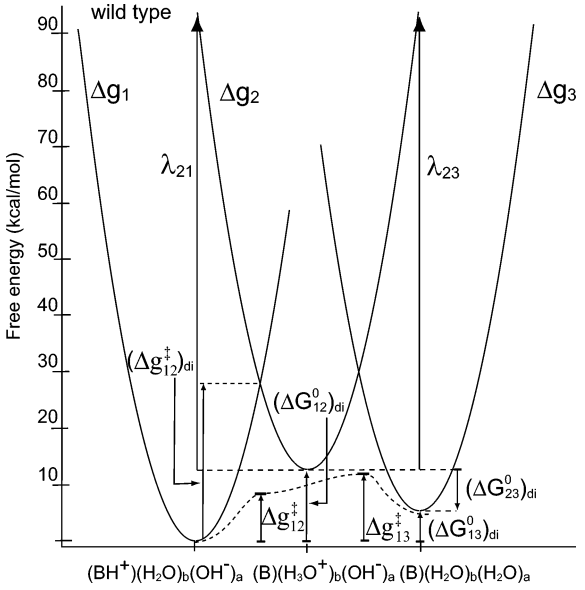

Figure 3. Three-state description of the PT in CA III for a case where the transfer involves two water molecules.

$$\Delta G_{PT} \cong 2.3RT(pK_a^p(D) - pK_a^p(A)) + \Delta V_{QQ}/\epsilon(R) \quad (22)$$

where $\Delta V_{QQ}/\epsilon(R)$ is the change in effective charge−charge interaction between the donor and acceptor upon PT and ϵ is the effective dielectric constant for charge−charge interaction (at a charge separation distance R). Equation 22 has been found to be valid even in cases where the donor and acceptor are in close proximity. Furthermore, even estimates without the last term give reasonable results due to the fact that the value of the function $\epsilon(R)$ is larger than 15 even at a distance of 3 Å (e.g., ref 48).

Just to set the problem in a clear way for further considerations we give in Figure 3 the potential surface for the wild-type enzyme using pK_a's of 5.0 and 9.0 for $(H_2O)_a$ and Lys64 (taken from ref 1) and pK_a = 0 for $(H_2O)_b$, evaluated by the PDLD/S−LRA method as described in the previous section.

With the model of eq 21 and with a reasonable estimate of the free energies ΔG_{12}^0 and ΔG_{23}^0 we can start to evaluate the apparent activation barrier. Before doing so we must clarify several points: (i) A Marcus-type relationship and the corresponding LFERs are *only* valid for a two-state system (1 → 2), that is, for a reaction with a single step. We have, however, a three-state process which involves a two-step mechanism (1 → 2 → 3). Fitting such a system to a Marcus-type formula can lead to nonphysical parameters (e.g., too small λ). (ii) To use the HAW approach in a three-state system (or in a four-state system), we must consider the elementary rate constants and then consider the pre-equilibrium concentrations, that is, the reaction

$$1 \underset{}{\overset{k_{12}}{\rightleftharpoons}} 2 \overset{k_{23}}{\rightleftharpoons} 3 \quad (23)$$

where $K_{12} = k_{12}/k_{23}$ involves the forward and backward rate constants k_{12} and k_{21} and $K_{23} = k_{23}/k_{32}$ involves the rate constants k_{23} and k_{32}. Note that k_{13} corresponds to k_{-B} in eq 2. We can fit the HAW equation to log k_{13} (or log k_B), but if we want to obtain the LFER for the 1 → 3 step we must take into account the free energy of state 2. More specifically let us consider the case when k_{23} is the rate-limiting step. In this case we would

TABLE 1: Estimating the Energetics (in kcal/mol) of PT Steps in Mutants of CA III[a]

	system	$pK_a(BH^+_{64})$	$pK_a(H_3O^+)_b$	$pK_a(H_2O)_a$	ΔG^0_{12}	ΔG^0_{23}	ΔG^0_{13}	$\Delta\Delta g^{\ddagger}_{obs}$	$\Delta\Delta g^{\ddagger}_{calc}$
α	wild-type	9.0	0	~5[b]	12.4	−6.9	5.5	0	0
i	K64H	7.5	0	4.3	10.3	−5.9	4.4	−1.8	−2
ii	K64H-R67N	7.5	−1.2	5.3	12.0	−9.0	3.0	−2.6	−1.5
iii	K64H-F198L	8.6	0	6.7	11.9	−9.2	2.7	−1.9	−2.0
iv	K64H-R67N-F198L	6.8	−1.2	6.8	11.0	−11.0	0	−3.4	−3.0
v	K64H-F198D	6.5	−0.5	8.4	9.7	−12.3	−2.6	−3.2	−3.3
vi	K64H-R67N-F198D	6.4	−1.7	8.7	11.2	−14.4	−3.2	−3.5	−3.0

[a] The pK_a's of $(H_2O)_a$ and BH^+_{64} are taken from ref 1 unless stated otherwise. [b] Estimated in ref 17.

have[18]

$$k_{13} = k_{23}(k_{12}/k_{21}) = k_{23}K_{12} \tag{24}$$

where K_{12} is the equilibrium constant for $1 \rightarrow 2$. Now we can write

$$\ln k_{12} = \ln(k_{23}) + \ln(K_{12}) \tag{25}$$

with $k_{ij} = (RT/h)\exp\{-\Delta g^{\ddagger}_{ij}/RT\}$ and $K_{ij} = \exp\{-\Delta G^0_{ij}/RT\}$ we obtain

$$\Delta g^{\ddagger}_{13} = \Delta g^{\ddagger}_{23} + \Delta G^0_{12} \tag{26}$$

Now using eq 5 we obtain

$$\begin{aligned}\Delta g^{\ddagger}_{13} &\cong \Delta G^0_{12} + [(\Delta G^0_{23} + \lambda_{23})^2/4\lambda_{23} - H'_{23}] + w \\ &= \Delta G^0_{12} + (\Delta g^{\ddagger}_{23})_{di} - H'_{23} + w\end{aligned} \tag{27}$$

where $H'_{12} = H_{12} + \Gamma$ and where we neglected for simplicity the H^2_{12} term in eq 5. If the rate-limiting step is $1 \rightarrow 2$, then k_{12} determines k_{13} and we can write

$$\begin{aligned}\Delta g^{\ddagger}_{13} = \Delta g^{\ddagger}_{12} &= (\Delta G^0_{12} + \lambda_{12})^2/4\lambda_{12} - H'_{12} + w \\ &= (\Delta g^{\ddagger}_{12})_{di} - H'_{12} + w\end{aligned} \tag{28}$$

Here we neglected for convenience the $(H')^2$ term in eq 5, since the corresponding correction is small in our case.

The formulation of eqs 27 and 28 should help one to explore the molecular origin of the observed LFER. Unfortunately, as is the case in many biological problems, it is almost impossible to obtain a unique result by fitting the observed dependence of log k_B on ΔG^0_{13} (or the corresponding ΔpK_a). For example, as will be shown below, the pK_a of $(H_3O^+)_b$ is not constant in the different mutants studied. Furthermore, the problem involves too many free parameters unless one uses computer simulation approaches to reduce the number of free parameters. Thus, we will take a different approach than that taken by Silverman and co-workers and we will augment our consideration by simulation studies.

In view of the complexity of eqs 27 and 28 we find it more convenient to try to reproduce the observed LFER by direct evaluation of these equations using the relevant calculated and observed parameters, with only minimal adjustment procedure. Our starting point is the estimate of ΔG^0_{12} and ΔG^0_{23} for the different mutants studied in ref 1. The relevant free energy values (Table 1) were obtained using the observed pK_a's of $(H_2O)_a$ and B_{64} and the calculated pK_a of $(H_2O)_b$. The PDLD/S−LRA calculations of this pK_a represented the effects of the charges of the protein ionized groups using a macroscopic approach as discussed in section II. The interaction with the charge of the zinc-bound hydroxyl ion $(OH^-)_a$ was treated explicitly in the PDLD/S−LRA calculations. This means that the last term in eq 22 was treated explicitly in our study of a PT between $(H2O)_a$ and $(H2O)_b$. We used the value $\lambda_{23} \cong 80$ kcal/mol obtained from the EVB simulations [2] as a generic value for both λ_{12} and λ_{23}. The value of $\bar{H}_{ij}(x^{\ddagger})$ was taken as 18 kcal/mol (which reflects a minor adjustment from the value found in ref 2) and $\bar{H}_{ij}(x_0)$ was taken as 10 kcal/mol from an EVB study of a proton transfer from $(H_2O)_a$ to $(H_2O)_b$. With the estimated ΔG_0, λ, and $\bar{H}_{ij}$ we evaluated the diabatic free energy functions and used them to obtain the corresponding $(\Delta\Delta g^{\ddagger})_{di}$ and $\Delta\Delta g^{\ddagger}$ for the mutants considered in Table 1. The corresponding graphical analysis is given in Figures 3−5, and the resulting dependence of $\Delta\Delta g^{\ddagger}$ on ΔG_{13} and the corresponding ΔpK_a's is given in Table 2 and Figures 4−7. As seen from the table and the figures, our model reproduced the observed trend. However, the origin of the trend is very different than that deduced from the two-state Marcus equation. That is, the flattening of the LFER at $\Delta pK_a > 0$, that would be considered in a phenomenological analysis of a two-state model as the beginning of the Marcus inverted region (where $\Delta G_0 = -\lambda$), is due to other factors. For example, the fact that $\Delta g^{\ddagger}$ does not change significantly upon moving from mutant iv to mutant vi, despite the increase in driving force (the reduction of ΔG^0_{13}) is due to the fact that the free energy of the intermediate state changes much less than that of the final state. In other words, the activation barrier for (vi) is not larger than that of (iv) despite the decrease in ΔG^0_{13} because ΔG^0_{12} and $\Delta g^{\ddagger}_{12}$ do not change significantly and thus limit the effect of the reduction in $\Delta g^{\ddagger}_{23}$. Thus, the trend in moving from (iv) to (v) is not due to having $\lambda \approx -\Delta G$ (this would require very small λ) but to the behavior of the three-state system.

At this stage it might be useful to clarify that the scheme of eq 21 can be easily extended to a system with one or more additional water molecules. To illustrate this point we consider the four-state case extension of eq 21. Here we may consider several limiting cases. In the first one $\Delta g^{\ddagger}_{12}$ is rate limiting. In this case we obtain eq 28 with $\Delta g^{\ddagger}_{14}$ replacing $\Delta g^{\ddagger}_{13}$. In the next case $\Delta g^{\ddagger}_{23}$ is rate limiting, so we obtain eq 27 with $\Delta g^{\ddagger}_{14}$ replacing $\Delta g^{\ddagger}_{13}$. Finally, we consider the case where $\Delta g^{\ddagger}_{34}$ is rate limiting. Then we obtain

$$\Delta g^{\ddagger}_{14} \cong \Delta G^0_{13} + \Delta g^{\ddagger}_{34} \tag{29}$$

Here $\Delta g^{\ddagger}_{34}$ is evaluated in a complete analogy to $\Delta g^{\ddagger}_{23}$ in eq 27.

Also, in the case of a four-state model it is easy to obtain the relevant energetics by calculation of the pK_a's of $(H_2O)_b$ and $(H_2O)_c$. A preliminary qualitative analysis produced a similar trend to that obtained for the three-state model. This reflects the fact that when we have an additional water its pK_a is not much different than that of $(H_2O)_b$, since it is located in a similar environment. Thus, the plateau of the surface in the regions where the proton moves from $(H_2O)_b$ to $(H_2O)_c$ does not change the overall trend, which is defined by the $1 \rightarrow 2$ and $3 \rightarrow 4$ steps. However, we do not feel that it is justified to perform a

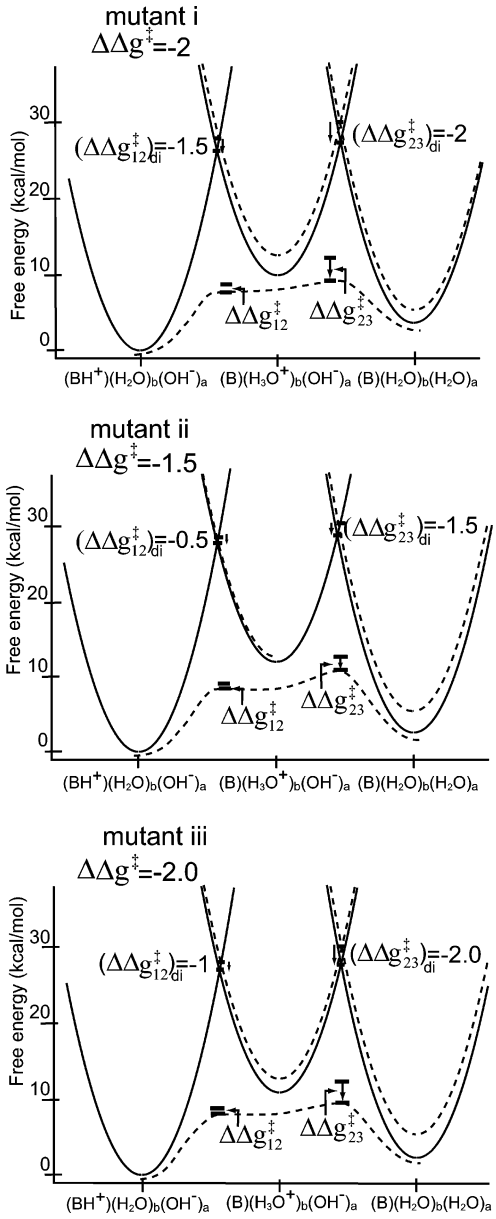

Figure 4. Analysis of the energetics of PT in the i, ii, and iii mutants of CA III. The figure describes the three states of eq 21 and considers their change in each of the indicated mutants (relative to the native enzyme). The figure displays the changes in the diabatic potential surfaces and the corresponding changes in the adiabatic activation barriers. The figure also gives the changes in the diabatic activation energies. The final activation barrier is taken in each case as the highest adiabatic barrier.

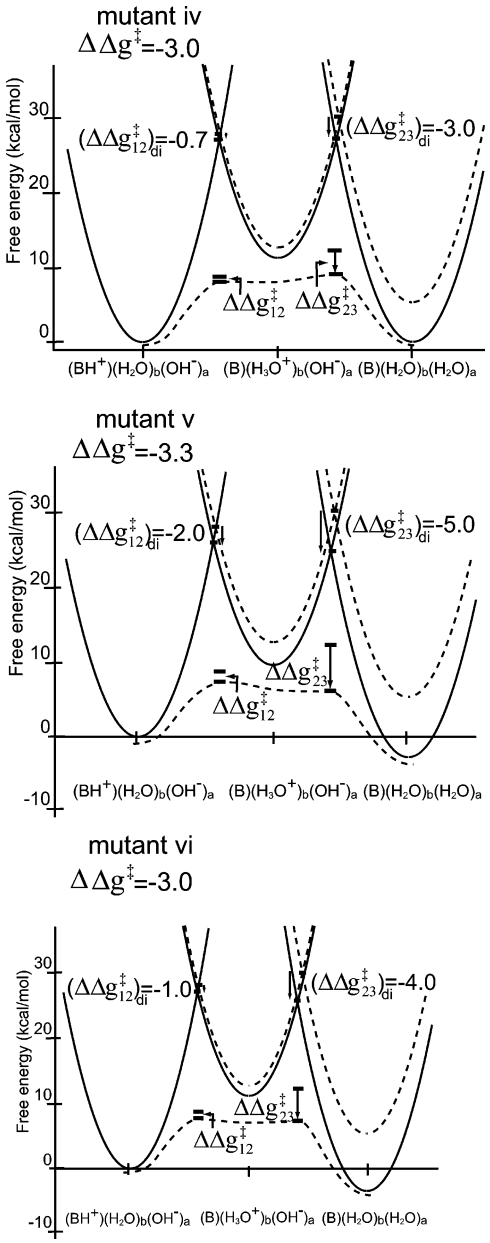

Figure 5. Analysis of the energetics of PT in the iv, v, and vi mutants of CA III. The notation is the same as in Figure 4.

full quantitative analysis in this stage. That is, the main purpose of the present paper is to provide a physically consistent analysis with physically consistent parameters and to relate it to the apparent results obtained from the much less consistent two-state model. We feel that a detailed discussion of the four-state model will be counterproductive in leading to more complex and thus less instructive results. We would also like to note that it costs quite a small amount of energy to bring $(H_2O)_b$ and B_{64} to an optimal distance for an efficient PT and thus to compete with a PT process that involves an additional water molecule.

With the above results in mind one might wonder about the possibility that the PT process is concerted. Recent studies[55,56] criticized the early EVB studies of the catalytic reaction of CA,[9,29] arguing that the PT process is concerted and that the agreement between the EVB and the experimental results may be coincidental. Here we would like to clarify first that the importance of the concerted mechanism has not been established properly. That is, at present all the theoretical support for a concerted PT (e.g., refs 55 and 56) has been based on gas phase models, rather than on proper calculations in the protein site. The use of gas phase ab initio models may give accurate gas phase results, but such models cannot be used to examine PT (or any other process) in proteins. It clearly cannot address the effect of the protein, which was taken into account consistently and reliably in the EVB studies.[9,29] Note that the EVB approach guarantees reliable results by calibrating the potential surface on the reference solution reaction. Furthermore, ab initio studies which include the surrounding environment in related PT processes (e.g., ref 57) have not found a special advantage for a concerted motion. Moreover, a proper examination of a concerted mechanism must compare its energetics to the energetics of a stepwise mechanism, and no such calculations have been yet reported for CA. It is also important to note that a very similar LFER is obtained for PT processes where the

TABLE 2: FER Analysis for Different Mutants of CA III[a]

	system	ΔG_{13}^0	ΔpK_a	$(\Delta\Delta g^{\ddagger})_{dia}$	$(\Delta\Delta g^{\ddagger})_{calc}$	$(\Delta\Delta g^{\ddagger})_{obs}$
α	wild-type	5.5	−4.0		0	0
i	K64H	4.4	−3.1	−2.0	−2	−1.8
ii	K64H-R67N	3.0	−2.2	−1.5	−1.5	−2.6
iii	K64H-F198L	2.7	−2.0	−2.0	−2.0	−1.9
iv	K64H-R67N-F198L	0	0	−3.0	−3.0	−3.4
v	K64H-F198D	−2.6	1.9	−3.3	−3.3	−3.2
vi	K64H-R67N-F198D	−3.2	2.3	−3.0	−3.0	−3.5

[a] Energies in kcal/mol.

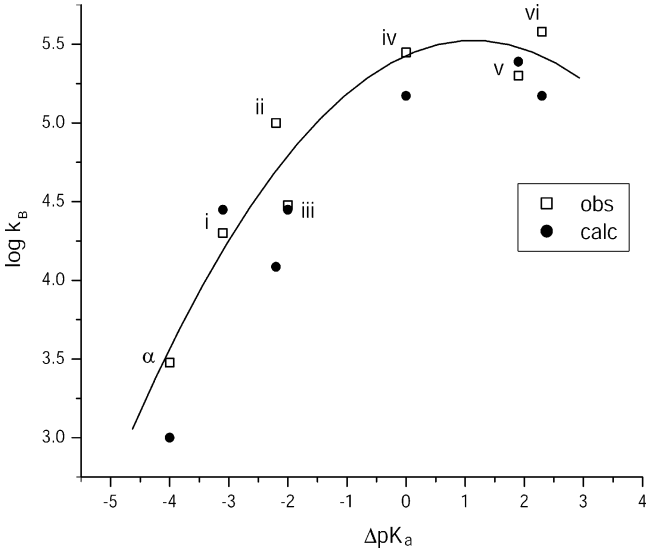

Figure 6. Calculated and observed FER for CA III. The different systems are marked according to the notation of Table 1. The term ΔpK_a corresponds to the pK_a difference between the zinc-bound water and the pK_a of the given donor group ($\Delta pK_a = -\Delta G_{13}/2.3RT$).

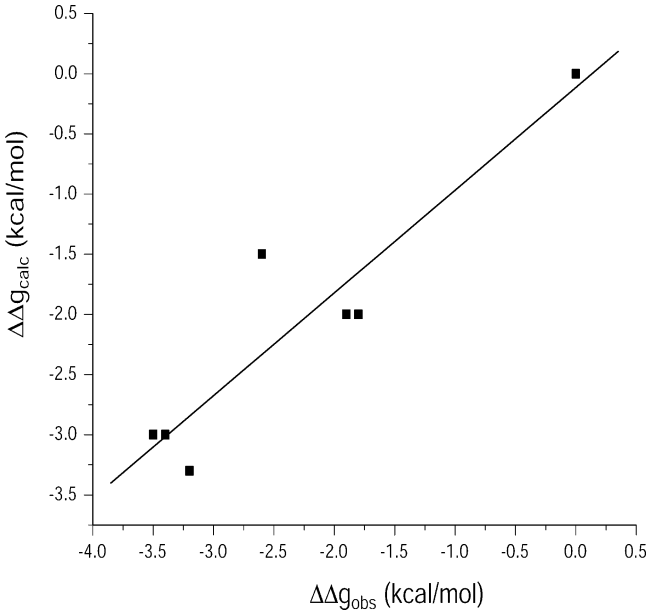

Figure 7. Correlation between the calculated and observed $\Delta\Delta g_{cat}^{\ddagger}$.

concerted and stepwise mechanisms have similar energetics. This reflects the fact that the energy of the concerted mechanism reflects the energy of the corners of the corresponding two-dimensional diagram (whose diagonal corresponds to the concerted mechanism). Thus, our analysis would be valid even if the concerted mechanism were to be found to have a somewhat lower barrier than that of the stepwise mechanism. Basically, the activation barriers of concerted mechanism are correlated with the energetics of the corresponding stepwise mechanisms. Finally, the rate-determining step that was studied in our EVB simulations (the PT from the zinc-bound water to the next water molecule) is the process that determines the overall PT process regardless if the subsequent steps are partially concerted.

It is also useful to comment about the suggestion that the observed isotope effect is consistent with a concerted mechanism.[55] This assertion involves two problems. First, consistent calculations of the kinetic isotope effect (KIE), that included all nuclear quantum effects and the dynamical effects of the protein,[2,22] reproduced the observed isotope effect, while exploring the PT in CA as a stepwise mechanism. The attempt of ref 55 to consider a concerted PT did not involve any comparison of the difference between the isotope effects of concerted and stepwise mechanisms. More importantly, this study did not consider the effect of the protein. Basically, a proper analysis of the relationship between isotope effects and the nature of the corresponding potential surfaces is much more involved than what is usually implied in the field. In fact, the customary idea that isotope effects can be used to establish concerted mechanisms[58,59] has been found to be an oversimplification.[57,60] In our view, only careful simulations that consider isotope effects in different mechanistic options can provide a unique interpretation of these effects and their relationship to the corresponding potential surfaces.

V. Concluding Remarks

The present work reexamined the origin of the observed LFER in CA III. This was done by a rigorous examination of the free energy profiles obtained from an EVB treatment of several VB states, which correspond to several intersecting parabolas. This treatment reduces to the Marcus relationship in the case of two intersecting parabolic surfaces and small H'_{ij}. Our analysis reproduced the observed LFER without using adjustable parameters, while providing results that were quite different than those obtained by fitting a simple Marcus relationship to the observed LFER. First, it was found that once we used a multiparabolas analysis, the work function, w^r, became negligible. The parameter w^r may be large in processes that involve the entropy of bringing the donor and acceptor together. However, in the case of CA III the donor and acceptor are more or less fixed and w^r is expected to be small. In fact, any local orientation of the donor and acceptor during the proton transfer process may be captured by λ rather than by w^r. Second, it was found here that the observed LFER can be reproduced by the HAW treatment, with significant H_{ij} and with the realistic λ's obtained from molecular simulation. This λ is much larger than the λ obtained by fitting λ_{in} to the two-state Marcus relationships (80 kcal/mol vs 5.6 kcal/mol). Now in considering the more realistic λ obtained from the simulations (see the discussion below of the issue of realistic estimates of λ) it is important to realize that λ is composed of "inner sphere" solute contribution,

λ_{in}, and an "outer sphere" protein−solvent contribution, λ_{out}. That is, we can decompose λ to

$$\lambda = \lambda_{in} + \lambda_{out} \tag{30}$$

The value of λ_{in} is strongly correlated with the value of H_{ij} since the nature of the solute diabatic state is not unique (the gas phase ab initio surface of the solute can be fitted with different λ_{in} and different H'_{ij}). In general, smaller λ_{in} is obtained with smaller H'_{ij}. However, the main issue here is the value of λ_{out}. This value, that reflects the protein contribution, has been evaluated by a stable and rigorous approach which was verified and quantified in many studies (e.g., refs 6, 19, and 61). Obviously, using this approach and reproducing the observed LFER with a correct multistate EVB model is more informative and much more physically consistent than an empirical deduction of λ from Marcus' formula.

The extraction of λ from fitting eq 4 to the observed LFER requires that $\lambda = -\Delta G^0$ so that $\Delta G^0 < 0$ in the point where the LFER becomes flat. This means that we must have data from regions where $\Delta G^0 < 0$. However, at least for the cases when $\Delta g^{\ddagger}_{12}$ is rate limiting, ΔG^0_{12} cannot be negative and the observation of a beginning of a flat LFER is actually due to other factors (see section III). It is also important to realize that λ_{out} cannot become too small and never approaches zero, which is the continuum limit for a completely nonpolar environment (see the discussion in ref 19). The reason is quite simple; the protein cannot use a nonpolar environment because this will decrease drastically the pK_a of $(H_3O^+)_b$. Instead, proteins use polar environments with partially fixed dipoles. However, no protein can keep its dipoles completely fixed (the protein is flexible) and thus give a non-negligible λ_{out}. Of course, this reorganization energy is still smaller than the corresponding value for proton transfer in solutions, but it never approaches the low value obtained from fitting in a two-state Marcus formula.[16,62]

As long as we obtain the value of H'_{ij} from fitting to observed LFERs, it is possible to argue that both eqs 3 and 5 reflect a phenomenological fitting with a free parameter (w and λ in the case of eq 3 and H'_{ij} in the case of eq 5). The difference, however, is that eq 5 and the use of three free energy functionals reflect much more realistic physics. This is evident, for example, from the fact that with eq 5 we do not obtain an unrealistically large w^r. Note in this respect that ΔG^0_{12} in eq 27 might look like w in a phenomenological fitting to the Marcus equation. It is also important to emphasize at this point that the present treatment is not a phenomenological treatment with many free parameters, as might be concluded by those who are unfamiliar with molecular simulations. That is, our approach is based on realistic molecular parameters obtained while starting from the X-ray structure of the protein and reproducing the relevant pK_a's and reorganization energy. Reproducing the observed LFER by such an approach, without adjusting the key parameters, is fundamentally different than an approach that takes the observed LFER and adjusts free parameters in a given model to reproduce it. In such a case one can reproduce any experiment by almost any model.

As explained in the previous section, the Marcus-like behavior of the observed LFER is not due to the transition to the Marcus inverted region (this would require a very small λ) but to the change in the energy of the intermediate state. That is, at high driving force (moving from (iv) to (vi) through (v)) the overall rate increases and then starts to decrease since k_{12} becomes now the rate-limiting step (see Figures 4 and 5).

It seems to us that there is no need for an experimental "proof" of the fact that the system cannot be described as a one-step model. We also consider the requirement for an experimental "proof" of the validity of eq 5 similar in some respect to the requirement of an experimental proof of the validity of the quadratic equation (which is simply a mathematical fact). That is, a requirement for a proof of the validity of a given LFER would be reasonable for phenomenologically based equations, but it is less justified for relationships that are obtained from fully microscopic approaches. The difference is that with a fully microscopic approach we can evaluate λ by basically a first-principle approach, as is now recognized in the electron transfer community (e.g., see refs 33 and 63). This is crucial since direct measurements of λ are very challenging. Fortunately, however, calculations of λ are expected to be quite reliable so that λ should not be considered as an adjustable parameter.

At any rate, since it is always more convincing to provide experimental proofs, it would be useful to illustrate the validity of our approach by mutation experiments. Since mutation experiments will mainly change λ and ΔG^0, it is conceivable that one can reach a range where eq 3 does not reproduce the observed LFER. In fact, it is hard to reproduce the experimental trend by eq 3 while requiring that $w^r \rightarrow 0$, and it is hard to find a physical justification for using a large w^r. It will also be very useful to create mutants where the site of $(H_2O)_b$ is replaced by a residue with an apparent pK_a of about 3 or 4. This will push down the energy of the intermediate state and accelerate the reaction.

It might be useful to address here the possible perception that the extensive and instructive experimental studies of PT in solutions have provided quantitative estimates of the solvent reorganization energy in PT processes and that somehow our studies contradict these experimental findings. In fact, we are not aware of any proper experimental evaluation of λ in PT reactions, since λ is completely defined by the diabatic states, which are not available experimentally. Furthermore, the solvent (or protein) contribution to λ is also not available experimentally. It is also useful to point out in this respect that λ is not equal to $4\Delta g^{\ddagger}$ when $\Delta G^0 = 0$, as can be assumed from the Marcus relationship. The reason is, of course, the effect of H_{12}. Thus, calculations that give $\Delta G^0 = 0$ for some PT steps in CA, as is the case in our calculations for the $2 \rightarrow 3$ step and in some steps in ref 56, do not provide any direct information about λ. Apparently, the most reliable estimates of λ are obtained by microscopic simulations (see above). This means that the small λ values obtained from eq 3 are unrealistic and should not be used in analyzing the origin of enzyme catalysis.

Finally, it is useful to comment about the general issue of proton transport in proteins. We consider the present study as a useful verification of our recent approach for simulating PT in bacterial reaction centers (RCs)[23] and in ref 64. This approach was based on the use of eq 5 and on evaluation of the relevant pK_a's by the PDLD/S−LRA approach. One of the main points of this study was the demonstration that PT processes are controlled by the pK_a's of the elements in the proton conduction chain (water and ionizable amino acids) and not by the minor effects of hydrogen bond orientation or degree of concreteness. More specifically, the problem with the oversimplified picture of "proton wires"[56,65] is that it focuses on relatively small factors such as orientations of the donor and acceptor and completely overlooks the key role of the energetics of forming a charged group (e.g., H_3O^+) in different environments. These energetics determine and control the overall barrier for the proton transport process.[23,45,64] Our point of view is supported by the present study where, for example, the $\Delta g^{\ddagger}_{32}$ barrier is determined by

the energetics of forming the $(OH^-)_a-(H_3O^+)_b$ pair and not by their specific distance or orientation (the donor and acceptor can easily reach an optimal distance).

Acknowledgment. This work was supported by NIH Grant GM-40283. Computer support was provided by the High Performance Computing and Communication Center (HPCC) of the University of Southern California.

References and Notes

(1) Silverman, D. N.; Tu, C.; Chen, X.; Tanhauser, S. M.; Kresge, A. J.; Laipis, P. J. *Biochemistry* **1993**, *34*, 10757−10762.
(2) Warshel, A.; Hwang, J. K.; Åqvist, J. *Faraday Discuss.* **1992**, *93*, 225−238.
(3) Hammett, L. P. *Physical Organic Chemistry; Reaction Rates, Equilibria, and Mechanisms*; McGraw-Hill Book Company: New York, 1970.
(4) Maskill, H. *The Physical Basis of Organic Chemistry*; Oxford University Press: Oxford, U.K., 1985; Chapter 10.
(5) Albery, W. J. *Annu. Rev. Phys. Chem.* **1980**, *31*, 227−263.
(6) Kong, Y. S.; Warshel, A. *J. Am. Chem. Soc.* **1995**, *117*, 6234−6242.
(7) Marcus, R. A. *J. Chem. Phys.* **1968**, *72*, 891.
(8) Hwang, J. K.; King, G.; Creighton, S.; Warshel, A. *J. Am. Chem. Soc.* **1988**, *110*, 5297−5311.
(9) Åqvist, J.; Warshel, A. *Chem. Rev.* **1993**, *93*, 2523−2544.
(10) Warshel, A. *Computer Modeling of Chemical Reactions in Enzymes and Solutions*; John Wiley & Sons: New York, 1991.
(11) Shaik, S. S.; Schlegel, H. B.; Wolfe, S. *Theoretical Aspects of Physical Organic Chemistry. The SN_2 Mechanism*; John Wiley & Sons: New York, 1992.
(12) Fersht, A. R.; Leatherbarrow, R. J.; Wells, T. N. C. *Nature* **1986**, *322*, 284.
(13) Warshel, A. Simulating the Energetics and Dynamics of Enzymatic Reactions. In *Specificity in Biological Interactions*; Proceedings of a Working Group of the Pontificiae Academiae Scientiarum Scripta Varia, Nov 9−11, 1983; Chagas, C., Pullman, B., Eds; Reidel Publishing Co.: Boston, MA, 1984; Vol. 55.
(14) Hawkinson, D. C.; Pollack, R. M.; Ambulos, N. P., Jr. *Biochemistry* **1994**, *33*, 12172−12183.
(15) Schweins, T.; Geyer, M.; Scheffzek, K.; Warshel, A.; Kalbitzer, H. R.; Wittinghofer, A. *Nat. Struct. Biol.* **1995**, *2*, 36−44.
(16) Gerlt, J. A.; Gassman, P. G. *J. Am. Chem. Soc.* **1993**, *115*, 11552−11568.
(17) Silverman, D. N. *Biochim. Biophys. Acta.* **2000**, *1458*, 88−103.
(18) Schweins, T.; Warshel, A. *Biochemistry* **1996**, *35*, 14232−14243.
(19) Muegge, I.; Qi, P. X.; Wand, A. J.; Chu, Z. T.; Warshel, A. *J. Phys. Chem. B* **1997**, *101*, 825−836.
(20) Albery, W. J.; Knowles, J. R. *Biochemistry* **1976**, *15*, 5627−5631.
(21) Åqvist, J.; Feierberg, I. *Biochemistry* **2002**, *41*, 15728−15735.
(22) Hwang, J.-K.; Warshel, A. *J. Am. Chem. Soc.* **1996**, *118*, 11745−11751.
(23) Sham, Y.; Muegge, I.; Warshel, A. *Proteins: Struct., Funct., Genet.* **1999**, *36*, 484−500.
(24) Lindskog, S.; Engberg, P.; Forsman, C.; Ibrahim, S. A.; Jonsson, B.-H.; Simonsson, I.; Tibell, L. *Ann. N.Y. Acad. Sci.* **1984**, *429*, 61−75.
(25) Silverman, D. N.; Lindskog, S. *Acc. Chem. Res.* **1988**, *21*, 30−36.
(26) Krebs, J. F.; Ippolito, J. A.; Christianson, D. W.; Fierke, C. A. *J. Biol. Chem.* **1993**, *268*, 27458.
(27) Silverman, D. N.; Lindskog, S. *Acc. Chem. Res.* **1988**, *21*, 30−36.
(28) Åqvist, J.; Fothergill, M.; Warshel, A. *J. Am. Chem. Soc.* **1993**, *115*, 631−635.
(29) Åqvist, J.; Warshel, A. *J. Mol. Biol.* **1992**, *224*, 7.
(30) Warshel, A.; Russell, S. T. *Q. Rev. Biophys.* **1984**, *17*, 283−421.
(31) Hwang, J.-K.; King, G.; Creighton, S.; Warshel, A. *J. Am. Chem. Soc.* **1988**, *110*, 5297−5311.
(32) Marcus, R. A. *Annu. Rev. Phys. Chem.* **1964**, *15*, 155.
(33) King, G.; Warshel, A. *J. Chem. Phys.* **1990**, *93*, 8682−8692.
(34) Warshel, A. *Annu. Rev. Biophy. Biomol. Struct.* **2003**, *32*, 425−443.
(35) Warshel, A.; Weiss, R. M. *J. Am. Chem. Soc.* **1980**, *102*, 6218−6226.
(36) Aqvist, J.; Warshel, A. *Chem. Rev.* **1993**, *93*, 2523−2544.
(37) Vuilleumier, R.; Borgis, D. *Chem. Phys. Lett.* **1998**, *284*, 71−77.
(38) Schmitt, U. W.; Voth, G. A. *J. Phys. Chem. B* **1998**, *102*, 5547−5551.
(39) Villa, J.; Warshel, A. *J. Phys. Chem. B* **2001**, *105*, 7887−7909.
(40) Schweins, T.; Geyer, T. M.; Kalbitzer, H. R.; Wittinghofer, A.; Warshel, A. *Biochemistry* **1996**, *35*, 14225−14231.
(41) Warshel, A.; Schweins, T.; Fothergill, M. *J. Am. Chem. Soc.* **1994**, *116*, 6, 8437.
(42) Warshel, A. Correlation between Structure and Efficiency of Light-Induced Proton Pumps. In *Methods in Enzymology*; Packer, L., Ed.; Academic Press Inc.: London, 1986; Vol. 127, pp 578−587.
(43) Warshel, A. *Acc. Chem. Res.* **2002**, *35*, 385−395.
(44) Sham, Y. Y.; Chu, Z. T.; Warshel, A. *J. Phys. Chem. B* **1997**, *101*, 4458−4472.
(45) Warshel, A. *Photochem. Photobiol.* **1979**, *30*, 285−290.
(46) Lee, F. S.; Chu, Z. T.; Warshel, A. *J. Comput. Chem.* **1993**, *14*, 161−185.
(47) Warshel, A.; Russell, S. T.; Churg, A. K. *Proc. Natl. Acad. Sci. U.S.A.* **1984**, *81*, 4785.
(48) Schutz, C. N.; Warshel, A. *Proteins: Struct., Funct., Genet.* **2001**, *44*, 400−417.
(49) Johnson, E. T.; Parson, W. W. *Biochemistry* **2002**, *41*, 6483−6494.
(50) Sham, Y. Y.; Muegge, I.; Warshel, A. *Biophys. J.* **1998**, *74*, 1744−1753.
(51) King, G.; Warshel, A. *J. Chem. Phys.* **1989**, *91*, 3647−3661.
(52) Lee, F. S.; Warshel, A. *J. Chem. Phys.* **1992**, *97*, 3100−3107.
(53) Mallis, R. J.; Poland, B. W.; Chatterjee, T. K.; Fisher, A. R.; Darmawan, S.; Honzatko, R. B.; Thomas, T. A. *FEBS Lett.* **2000**, *482*, 237−241.
(54) Warshel, A. *Biochemistry* **1981**, *20*, 3167−3177.
(55) Smedarchina, Z.; Siebrand, W.; Fernández-Ramos, A.; Cui, Q. *J. Am. Chem. Soc* **2003**, *125*, 243−251.
(56) Cui, Q.; Karplus, M. *J. Phys. Chem. B* **2003**, *107*, 1071−1078.
(57) Strajbl, M.; Florián, J.; Warshel, A. *J. Am. Chem. Soc.* **2000**, *122*, 5354−5366.
(58) Daggett, V.; Schröder, S.; Kollman, P. *J. Am. Chem. Soc.* **1991**, *113*, 8926−8935.
(59) Schowen, R. L. Molecular Structure and Energetics. In *Principles of Enzyme Activity*; Liebman, J. F., Greenberg, A. D., Eds.; VCH Publishers: Weinheim, Germany, 1988; Vol. 9.
(60) Åqvist, J.; Kolmodin, K.; Florian, J.; Warshel, A. *Chem. Biol.* **1999**, *6*, R71−R80.
(61) Hwang, J.-K.; Warshel, A. *J. Am. Chem. Soc.* **1987**, *109*, 715−720.
(62) Pollock, E. L.; Adler, B. J.; Pratt, L. R. *Proc. Natl. Acad. Sci. U.S.A.* **1980**, *77*, 49.
(63) Warshel, A.; Parson, W. W. *Q. Rev. Biophys.* **2001**, *34*, 563−670.
(64) Burykin, A.; Warshel, A. *Biophys. J.* **2003**, *85*.
(65) Nagle, J. F.; Mille, M. *J. Chem. Phys.* **1981**, *74*, 1367−1372.